Overview of a Generalized Numerical Predictor-Corrector Targeting Guidance with Application to Human-Scale Mars Entry, Descent, and Landing

Rafael A. Lugo[1]
NASA Langley Research Center, Hampton, VA 23681, USA

Richard W. Powell[2]
Analytical Mechanics Associates, Hampton, VA 23666, USA

Alicia D. Cianciolo[3]
NASA Langley Research Center, Hampton, VA 23681, USA

Recent advances in planetary entry guidance algorithms are motived by precision landing criteria for human-scale Mars missions and improved in-space computing capabilities. An NPC targeting guidance algorithm, originally developed for the Mars Surveyor Program 2001 Missions, has been modified and extended to permit a fully generalized, flexible, and robust approach to spacecraft aerocapture and EDL guidance design. This paper describes this generalized targeting NPC guidance (NPCG) and how its modifications enable its use in precision targeting for human missions. System modeling, trajectory propagation, and guidance segment definition and design are described. Finally, the NPCG capability and performance is demonstrated using a human-scale Mars entry, descent, and landing mission simulation.

I. Introduction

The current state of the art in Mars entry, descent, and landing (EDL) guidance is exemplified by the NASA Mars Science Laboratory (MSL) mission that landed in August of 2012. The MSL entry vehicle (approximately 2.4 t) utilized a variation of the Apollo entry guidance that used bank magnitude to control downrange and bank reversals to control crossrange, ultimately achieving a landing ellipse capability of 20 km by 7 km. Precision landing requirements for human-scale Mars vehicles (between 50 t and 60 t), however, include landing the vehicle within 50 m of the targeted landing site. Recent work has shown that achieving this scale of precision landing with low lift-to-drag (L/D) human-scale entry vehicles at Mars is in part enabled by advanced guidance and control schemes, including direct force control (DFC) and numerical predictor-correctors (NPC) [1]. An NPC targeting guidance algorithm, originally developed at NASA Langley Research Center for the Mars Surveyor Program 2001 Missions [2, 3], has been modified and extended to permit a fully generalized, flexible, and robust approach to spacecraft aerocapture and EDL guidance design. This paper describes this generalized targeting NPC guidance (NPCG) and how its modifications enable its use in precision targeting for human missions. Specifically, the single constraint requirement is replaced with a multi-dimensional targeting capability, and the use of bank reversals is replaced with direct control

[1] Aerospace Engineer, Atmospheric Flight and Entry Systems Branch, AIAA Member
[2] Aerospace Engineer, Atmospheric Flight and Entry Systems Branch, AIAA Fellow
[3] Aerospace Engineer, Atmospheric Flight and Entry Systems Branch, AIAA Senior Member

of angle of attack and sideslip. Additionally, opportunities to leverage advancements in flight computer hardware will be discussed. The NPCG performance is demonstrated in a simulated a human-scale Mars EDL case.

A. Nomenclature

The following parameters are used in this study. Their definitions are provided for clarification.

- *Control*: A variable within the NPCG that deliberately modifies the vehicle dynamics. In general, controls correspond to the commands the guidance issues to vehicle control systems. Examples include angle of attack, time of bank reversal, time of engine ignition, and engine throttle setting. A set of controls may be referred to as a control vector.
- *Constraint*: A variable within the NPCG with a specific value to be achieved via modulation of the controls. Also referred to as targets. Examples include landing site latitude/longitude/radius, energy at atmospheric exit, and range error at landing.
- *Segment*: A period during which the set of NPCG controls and constraints are fixed. In general, a trajectory is broken up by the user into segments that may (but not always) correspond to the various mission phases, such as entry, powered descent (PD), landing, etc. Each segment may use a different guidance methodology depending on the mission and vehicle. A new segment may begin before the vehicle actually reaches the propagated end of the current segment, that is, they may overlap.
- *Terminal Area Energy Management (TAEM)*: A guidance segment in which the controls and constraints are selected such that the vehicle energy is managed to target a specific segment termination condition. This TAEM segment is in contrast to a segment in which, for example, a g-load is targeted. The TAEM concept has its roots in Space Shuttle guidance development [4].

II. Generalized Numerical Predictor-Corrector Targeting Guidance

Consider a typical entry trajectory that begins at atmospheric interface and terminates at touchdown, such as that shown in Fig. 1 (note the logarithmic scale on both axes to emphasize the portion of the trajectory during PD). The vertical portion of the trajectory at left is terminal descent phase where the vehicle maintains a constant velocity. The trajectory is split into various segments, each of which have a particular set of controls that must be adjusted to achieve the constraints specified for that segment (see Section II.B for further details).

Targeting guidance algorithms manipulate the control vector (e.g., vehicle commands) during these segments such that the resultant trajectory satisfies specified requirements and constraints. Predictor-corrector algorithms achieve this by

1) generating a predicted vehicle trajectory given the current vehicle state and control vector (prediction),
2) comparing this trajectory against the constraints and computing the errors, and
3) calculating the required changes to the control vector that minimize those errors (correction).

In the case of the NPCG, the above process is achieved by

1) integrating the three degree-of-freedom (3DOF) translational equations of motion from the current navigated state to a specified termination point with the initial control vector (prediction), and
2) using a gradient-based targeting algorithm to determine the “best” control vector that satisfies the constraints for the current guidance segment (correction).

The converged control vector solution is commanded until the NPCG is called again. Command profiles are also supported. For example, the classical Apollo Powered Descent Guidance [5, 6] generates a desired acceleration vector profile that targets the desired landing site. The acceleration profiles are computed using polynomials, which in the case of the NPCG, would be calculated and passed as guidance commands until a new profile is generated.

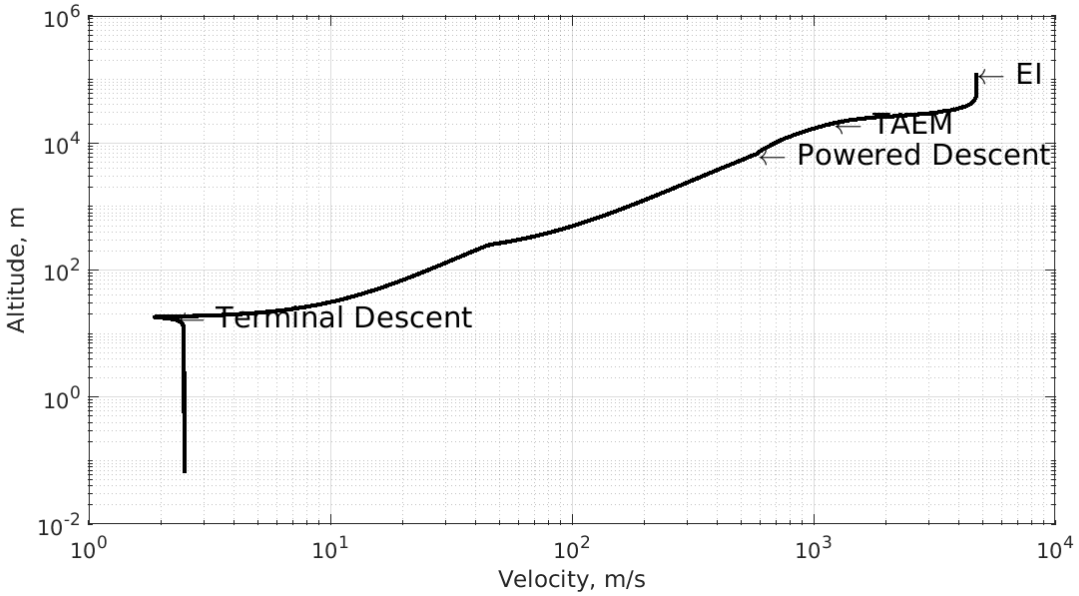

Fig. 1. Notional entry trajectory with notional guidance segments denoted. Note logarithmic scales on both axes.

A flowchart illustrating the logic flow of the NPCG is shown in Fig. 2. For any given segment, the trajectory waypoints, or targets, are defined and input. For example, a PD target might be the landing site coordinates. Further details of these segments are discussed in Section II.B. Other inputs to the NPCG include the current vehicle state provided by the navigation system and vehicle accelerations provided by the onboard inertial measurement unit (IMU). Estimates of atmospheric quantities can be provided by a flush air data system if so equipped [7].

The NPCG uses these inputs to update the current internal vehicle states and any available system models, such as aerodynamics, gravity, and atmosphere. These models are typically mission-dependent and are of a level of fidelity defined by the user, and are detailed further in Section II.A. The trajectory is then propagated to a specified termination point with these models and initial conditions using an algorithm detailed further in Section II.C. The targeting algorithm, described in Section II.B, is used in conjunction with the trajectory propagator to determine the control vector that provides the trajectory that best satisfies the constraints specified for that segment.

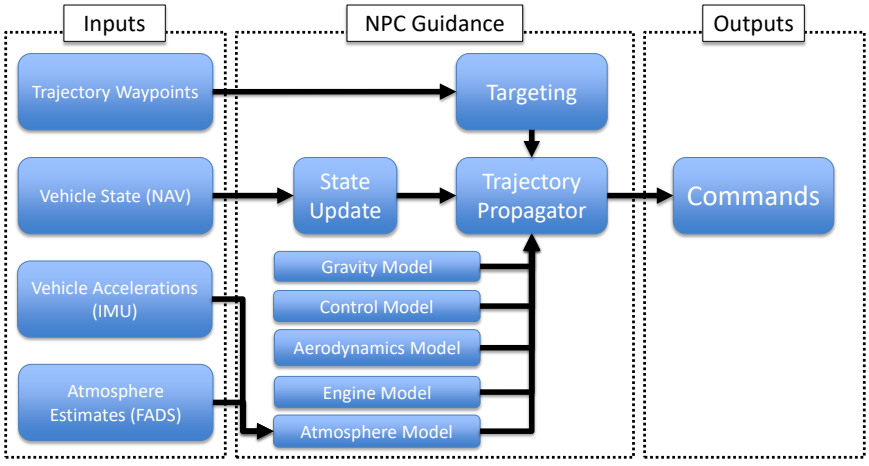

Fig. 2. Outline of a typical NPC guidance logic.

A. System Modeling

To permit accurate trajectory propagation, and therefore accurate trajectory predictions, the NPCG must include environmental and vehicle system models that provide the relevant forces acting upon the vehicle. For a notional human-scale Mars EDL mission, relevant models include:

- Gravity: Up to J8 spherical harmonic
- Aerodynamics: Nominal vehicle aerodynamic database
- Propulsion: Thrust and thrust direction relative to body frame, specific impulse (Isp), and rate-limited throttling
- Atmosphere: Mean Mars Global Reference Atmosphere Model (MarsGRAM) profile

1. Model Fidelity

The fidelity and accuracy of these internal NPCG models are such that without vehicle or atmospheric disturbances or perturbations, the propagated trajectories generated by the NPCG closely approximate the trajectory in the truth simulation (or, in actual flight, the trajectory that the vehicle flies). In this situation, the initial commands for a given segment generated by the NPCG are usually sufficient for the rest of the segment. In cases where disturbances or perturbations are present (such as in a more realistic trajectory simulation), or when some system or phenomena is not accurately modeled, the NPCG will continually make adjustments to the commands in an attempt to correct for those differences. This situation results in command "stair-stepping" as the NPCG "chases" the real vehicle dynamics that it is unable to model, until the command is saturated or the next segment is reached. In some cases, the internal guidance model fidelity may be insufficient to prevent stair-stepping in all dispersed conditions. However, the NPCG may still be able to recover in later segments. Care on the part of the trajectory and guidance designer must be taken to ensure that the as-flown trajectory is robust enough to these disturbances that the guidance and control (G&C) can compensate.

2. Vehicle Dynamics

Since the 3DOF equations of motion used by the NPCG only provide translational states, vehicle attitudes are computed using the commanded angles (for example, angle of attack or pitch angle). Generally, internal to the NPCG the vehicle always points in the commanded direction. However, since the true vehicle response is not instantaneous, the NPCG permits the user to input angular rate and acceleration limits so that changes in commanded angles result in vehicle attitude not changing instantaneously. If the user is careful in selecting these angular rate and acceleration limits, the 3DOF propagated trajectory internal to the NPCG can closely resemble the true vehicle dynamics.

3. Density Estimation

During atmospheric flight, the NPCG uses the sensed axial and normal accelerations from an on-board inertial measurement unit (IMU) to adjust the internal atmospheric density as well as axial and normal aerodynamic force models. In effect, the NPCG can update its models to reflect the estimated density, which results in more accurate propagated trajectories. This capability is especially effective for missions with poorly-known atmospheric conditions where density variations dominate the uncertainties.

B. Segment Definition

The segments, controls, and constraints are user-defined and depend on the mission, vehicle, control surfaces, planet, and targeting requirements. Table 1 lists example segments that make up the trajectory for a blunt body vehicle such as a capsule for two types of missions, aerocapture and EDL.

Note in particular that the constraints for at least two segments in both cases are the same: energy at atmospheric exit for aerocapture and landing site location for EDL. In the case of aerocapture, during the entry phase the trajectory is internally propagated to atmospheric exit, assuming a value for angle of attack during the exit phase (say 0°). If this exit phase angle of attack is carefully selected, control margin can be built into the system by forcing the NPCG to solve for the current (entry) angle of attack that will result in aerocapture given the exit angle of attack of 0°. When the vehicle reaches the time to switch to the next segment, only small angle of attack changes should be required since the guidance has already predicted what angle of attack during entry was needed such that the exit angle of attack was 0°. This scenario exemplifies how careful guidance segment design can improve system robustness. The case of EDL will be described in more detail in a later section.

Table 1. Example guidance segments for aerocapture and EDL.

Mission	Segment	Controls	Constraints
Aerocapture	Entry	• Angle of attack • Sideslip angle • Time of angle change • Exit angle of attack	• Energy at atmospheric exit • Wedge angle at atmospheric exit
	Exit	• Angle of attack • Angle of sideslip	• Energy at atmospheric exit • Wedge angle at atmospheric exit
EDL	Entry	• Angle of attack • Angle of sideslip	• Target energy at TAEM • Zero crossrange
	Terminal Area Energy Management (TAEM)	• Angle of attack • Angle of sideslip • Time of engine ignition	• Landing site latitude • Landing site longitude • Landing site radius
	Powered Descent	• Angle of attack • Angle of sideslip • Net engine throttle	• Landing site latitude • Landing site longitude • Landing site radius

C. Trajectory Propagation

Trajectories are propagated in the NPCG from the current vehicle state to an end point specified by the user. This end point can be landing, an intermediate point along the trajectory, or any variable space computable by the NPCG (e.g., time, altitude, propellant remaining, etc.).

The vehicle state is defined by the vector

$$\mathbf{x} = \begin{bmatrix} t & \mathbf{r} & \mathbf{v} & w \end{bmatrix} \tag{1}$$

where t is time, $\mathbf{r}$ is the inertial position vector, $\mathbf{v}$ is the inertial velocity vector, and w is the vehicle weight. The state derivatives with respect to time are then

$$\dot{\mathbf{x}} = \begin{bmatrix} 1 & \mathbf{v} & \mathbf{a} & \dot{w} \end{bmatrix} \tag{2}$$

which are computed using the 3DOF equations of motion and integrated using the classical fourth-order Runge-Kutta technique. The inertial acceleration vector $\mathbf{a}$ is computed using the sum of accelerations due to aerodynamic forces, accelerations due to engine thrust, and acceleration due to gravity:

$$\mathbf{a} = \mathrm{C}^{b \to i}\mathbf{a}_{aero} + \mathrm{C}^{b \to i}\mathbf{a}_{thrust} + \mathbf{g} \tag{3}$$

where C is the direction cosine matrix describing the transformation from the body frame b to the inertial frame i. The weight derivative is computed assuming that mass losses are due to thrusting engines consuming and expelling propellant.

D. Constraint Satisfaction

In a given segment, the NPCG determines the set of controls that satisfy the user-specified constraints for the remainder of the propagated trajectory. For example, an engine throttle setting that enables the vehicle to reach zero velocity a specified radius, to within a given tolerance, may be desired. To that end, a projected gradient algorithm (PGA) is used to determine the best set of multidimensional controls that satisfies the constraints for that segment. The PGA used by the NPCG is derived from that in the Program to Optimize Simulated Trajectories II (POST2) [8], which employs Rosen's projection method for nonlinear programming [9, 10, 11]. Use of pseudoinverse in the PGA permits solutions to overdetermined problems. Thus, multiple controls and constraints may be specified in any segment.

If the constraints are not satisfied, the NPCG will use the results from the best (i.e., lowest-weighted average error) trajectory. This condition typically occurs when the vehicle is close to the propagation endpoint and the sensitivity matrix used by the PGA becomes ill-defined. In these situations, the NPCG can still recover and re-converge later in the trajectory. In some cases, later segments can "correct" for inaccurate targeting in previous segments to a certain extent, such as PD correcting for errors accumulated during the entry phase. In general, however, the greater the errors, the greater the impact on performance if the vehicle recovers.

Notably, the PGA implementation in the NPCG does not include the cost-reduction function feature in POST2 that enables optimization; it only attempts to satisfy the constraints.

1. Scaling and Multithreading

While the PGA does not have an explicit limit to the number of controls or constraints (recall from Section II.B that the number of controls may be greater than or equal to the number of constraints), in general an observed best practice is to limit these to less than five to prevent the computation time from becoming excessive and precluding use on an actual flight computer. This limitation is due to the need to construct the sensitivity matrix, that is, to produce the Jacobian, the PGA perturbs each control by an increment defined by the user, integrates the equations of motion to the next segment or target, and calculates the partial derivative. If the user specifies a two-sided derivative, this process is repeated for the negated increment. Thus, for n controls, the PGA can propagate up to $2n+1$ trajectories (the 1 being the unperturbed case). Because the user can also specify the maximum number of iterations m, the number of propagated trajectories can be $m*(2n+1)$.

It is expected that advances in space- and human-rated computing hardware, specifically with multithreading, may significantly improve the NPCG performance and ability to handle higher quantities of controls and constraints because these trajectories are not dependent on each other and may be computed simultaneously.

III. Application: Human-Scale Mars Entry, Descent, and Landing

To demonstrate the NPCG guidance, the case study of a human-scale Mars entry vehicle utilizing a hypersonic inflatable aerodynamic decelerator (HIAD) is examined [12]. Control of the vehicle dynamics during entry is provided by four aerodynamic flaps, shown in Fig. 3 (note the lower flap is partially deployed). Control of the vehicle dynamics during PD is provided by eight 100 kN supersonic retropropulsion (SRP) main engines arranged in a doublet configuration. SRP is an approach that uses powered flight rather than more traditional parachute to reduce velocity during the descent and landing phases of EDL. If the engines are configured in such a way that they permit differential throttling or gimbaling, vehicle control authority during powered flight is enabled, and the NPCG can determine the time to start the engines, throttle setting, and thrust vector orientation.

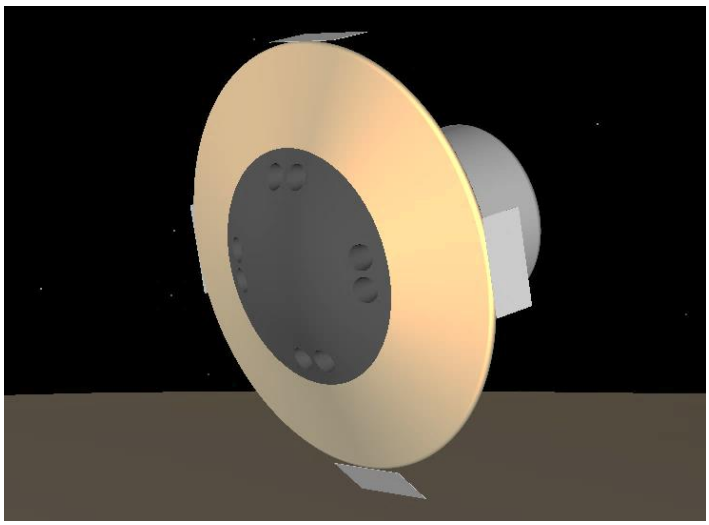

Fig. 3. Representation of the HIAD entry vehicle.

A. Concept of Operations

The crewed entry vehicle performs a deorbit burn at apoapsis of a 1 Sol polar orbit (33793 km apoapsis altitude by 250 km periapsis altitude). The polar orbit was chosen for the study because it permits access to any landing site on Mars. After the deorbit burn, the vehicle coasts until atmospheric entry interface (125 km altitude), at which point the simulation atmosphere and aerodynamic models are activated. The G&C algorithms are activated when the sensed vehicle acceleration reaches 0.15 g's. Throughout entry, DFC is utilized by the NPCG, which commands angles of attack and sideslip to control downrange and crossrange errors, respectively. At PD initiation (PDI), the main engines are activated and the vehicle begins the PD main phase using an augmented gravity turn through the use of differentially throttled main engines. The PD terminal phase occurs when the vehicle is directly over the landing site and descends vertically at a constant velocity of 2.5 m/s for 5 s. The EDL concept of operations is shown in Fig. 4.

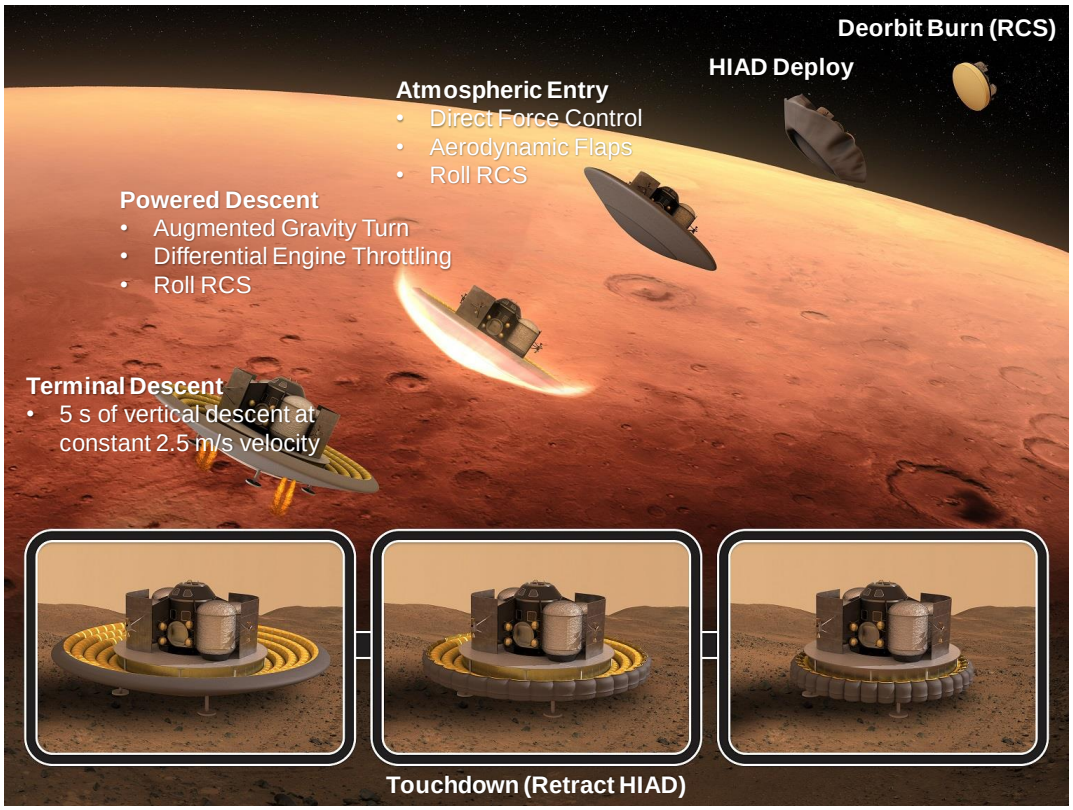

Fig. 4. Human-scale Mars EDL with HIAD vehicle.

B. Guidance Segments

The controls are picked such that the entry vehicle uses DFC in the form of angle of attack and sideslip commands to manage landing site targeting errors during entry. During PD, the time of engine ignition and net engine thrust are added to the controls. Table 2 shows the different controls and constraints for each guidance phase.

Table 2. NPC guidance segments for human-scale Mars EDL with HIAD vehicle.

Segment	Update (Hz)	Start Condition	End Condition	Propagation End	Controls	Targets (at Propagation End)
1	0.2	Sensed G Load	TAEM Acquisition	TAEM Acquisition	• Angle of attack • Angle of sideslip	• Energy at TAEM • Zero crossrange
2	0.2	TAEM Acquisition	PDI	Terminal Phase	• Angle of attack • Angle of sideslip • Time of PDI	• Landing site radius+12.5 m • Landing site latitude • Landing site longitude
3	1.0	PDI	Throttle Down	Terminal Phase	• Angle of attack • Angle of sideslip • Net engine thrust	• Landing site radius+12.5 m • Landing site latitude • Landing site longitude
4	1.0	Throttle Down	Terminal Phase	Landing	• Velocity at throttle down • Throttle setting at throttle down	• Pitch angle at terminal descent • Landing site radius
5	1.0	Terminal Phase	Landing	Landing	--	--

Recall from Section II.C that the targets for multiple segments can be the same, that is, segments can overlap. Consider segments 2 and 3 (TAEM and PD main phase), both of which propagate predicted trajectories down to the start of the PD terminal phase, which is 12.5 m above the landing site. When the vehicle is in TAEM, the internal predicted trajectory assumes a pure gravity turn during PDI, meaning that the vehicle is commanded at a zero angle of attack and sideslip with a constant thrust. This means that the NPCG is forced to solve for the TAEM angle of attack, sideslip, and time of PDI that targets the PD terminal phase with a pure gravity turn. Once PDI is initiated (the

NPCG enters segment 3), the controls still include angle of attack and sideslip. This is so that during PD, small errors built up during entry can be corrected by pointing the thrust vector off of the velocity vector. Since the NPCG has flown all of entry assuming a pure gravity turn, the angle of attack and sideslip commanded during PD is generally small (<5°). This is called an augmented gravity turn.

C. Monte Carlo Analysis

Monte Carlo analyses were performed using the dispersions listed in Table 3. The 'dusttau' listed is a measure of the dust loading in the atmosphere and has a significant impact on the density profile. Therefore, it is included in the Monte Carlos in addition to the nominal dispersions.

Table 3. Monte Carlo dispersions.

Category	Parameter	Dispersion	Distribution
Initial Conditions	Deorbit burn execution	0.135 m/s 3σ	normal
	Uncorrelated state covariance	0.03º 3σ for angles, 0.03 km 3σ for altitudes	normal
Atmosphere	Density	MarsGRAM	--
	Winds	MarsGRAM	--
	Dusttau	0.1:0.9	uniform
Aerodynamics	Aerodatabase uses coefficient multipliers and adders for different aerodynamic regimes based on CFD, wind tunnel tests, and flight data from similar shapes	--	--
Propulsion	Peak thrust	Scale factor: 1% 3σ	normal
	Peak Isp	Scale factor: 1% 3σ	normal
	Start lag time	0.0:0.2 s	uniform
	Startup transient rate	Scale factor: 1% 3σ	normal
	Main phase response rate	Scale factor: 1% 3σ	normal
Mass	Mass	500 kg 3σ	normal
	Center of gravity	0.05 m 3σ	normal
	Moments of inertia	5% kg-m^2 3σ	normal

IV. Results

Six-degree-of-freedom (6DOF) trajectories were simulated in the Program to Optimize Simulated Trajectories II (POST2), an event-driven, point-mass trajectory simulation software with discrete parameter targeting and optimization capability. The NPCG was implemented such that guidance commands were issued at a frequency of 0.2 Hz during entry and 1 Hz during PD. The NPCG models used were those listed in Section II.A, with a J2 gravity model rather than J8. Statistics from the Monte Carlo analysis are shown in Fig. 5 to demonstrate overall vehicle performance, specifically, a propellant usage 3σ value of approximately 1 t, and a landing accuracy of 33 m in a 99%-tile sense.

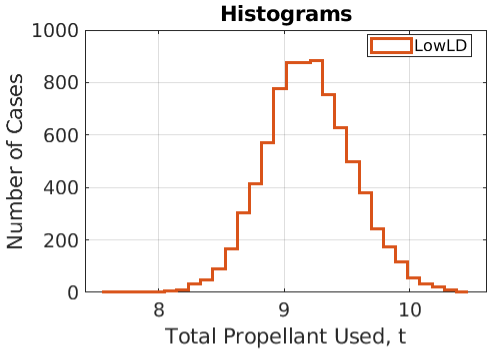

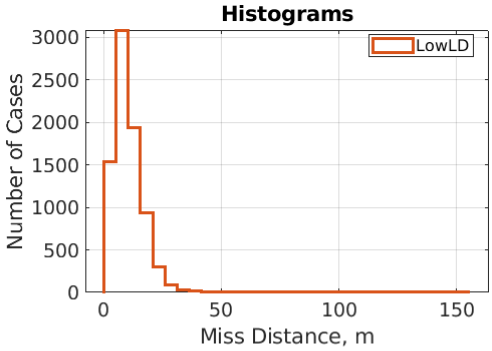

	LowLD
Mean	9.2
1-sigma	0.35
3-sigma	1.051
1.00 %-tile	8.396
99.00 %-tile	10.064
Max Value	10.444
Min Value	7.63
Percentage	99.5

	LowLD
Mean	10.626
1-sigma	7.684
3-sigma	23.052
1.00 %-tile	1.156
99.00 %-tile	33.047
Max Value	155.184
Min Value	0.003
Percentage	99.5

Fig. 5. Monte Carlo results, low L/D human-scale Mars EDL.

Fig. 6 illustrates how the different NPCG segments defined for this problem overlap and how the NPCG can self-correct. For this figure, the nominal case was run with the NPCG being called once at the beginning of each segment, rather than 0.2 Hz. Thus, once the NPCG PGA converges on a control vector solution, those command values are used for the remainder of the segment. Recall from Table 2 that segment 1 spans entry to TAEM acquisition, segment 2 spans TAEM acquisition to terminal descent, and segment 3 spans PDI to terminal descent.

The large (-9° to 3°) variation in angle of attack prior to G&C activation at 90 s due to the attitude drift of the vehicle as it enters the sensible atmosphere, but before the sensed acceleration reaches 0.15 g's. Once this g-load is reached, the NPCG and flap controller are activated, and the guidance converges on a solution of approximately -6° for segments 1 and 2. Also note that the change in command at the start is not instantaneous, but is rate- and acceleration limited to more closely approximate the true vehicle response. At this low dynamic pressure the internal NPCG dynamics approximation is significantly faster, but as the dynamic pressure increases, the NPCG better approximates the truth dynamics.

Notice the command in segment 2 increases from -6° to 0°, but the actual vehicle response is approximately -2°. Recall that segment 2 is designed to fly PD with a pure gravity turn, meaning that it will command a 0° angle of attack and sideslip. Once segment 3 is reached, meaning the vehicle engines are activated and powered descent is initiated, the NPCG computes a new control vector assuming an augmented gravity turn, meaning that the guidance is now permitted to use angle of attack and sideslip during PD to clean up any errors accumulated during entry. Thus, for this nominal case where only a single command vector is computed for each segment, the NPCG determined that a -2° angle of attack was required during PD to target the landing site. This illustrates how segment and control vector choices can influence how margin can be built into the system, by permitting later segments to correct errors built up in earlier segments.

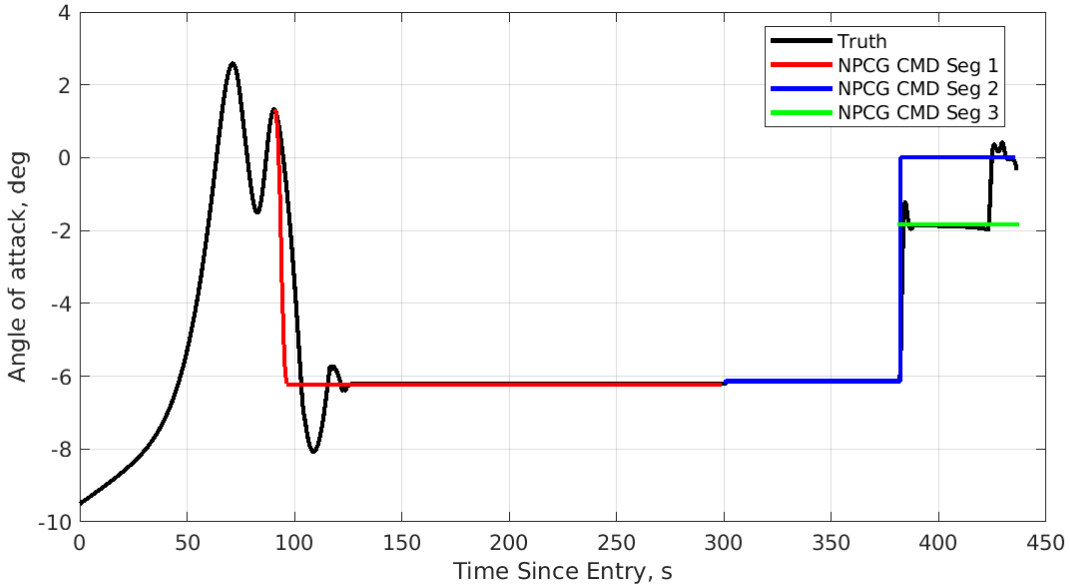

Fig. 6. NPCG command and vehicle response, nominal case, single NPCG call.

Subsequent figures show how the guidance commands change between the nominal and a selected dispersed trajectory. In these cases, the NPCG is called at a rate of 0.2 Hz during entry rather than once as in Fig. 6. In general, the nominal case exhibits less variability, which is by design. The dispersed case exhibits more variability, indicating that the guidance is making corrections to the angle and thrust commands to be able to fly out the targeting errors. In both cases, the vehicle lands within a few meters of the targeted landing site. The nominal case lands using a total of 9.58 t of propellant, while the dispersed case lands using a total of 9.22 t of propellant.

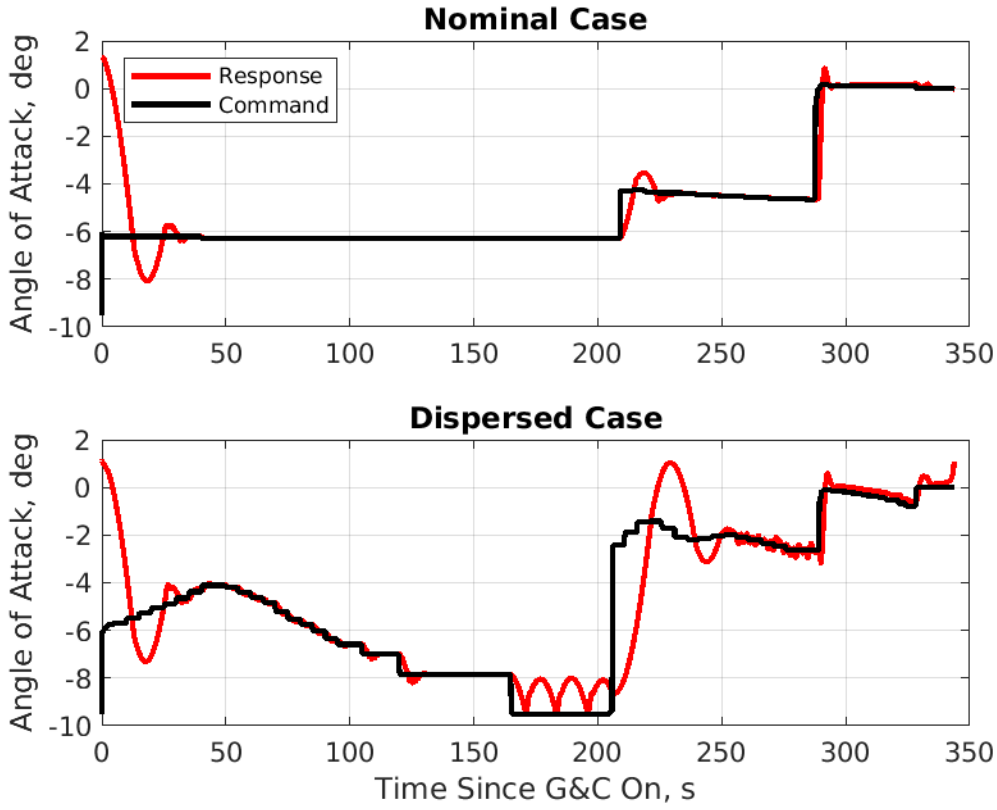

Fig. 7. Nominal and dispersed angle of attack commands and responses during entry and PD.

Fig. 7 shows the nominal and dispersed angle of attack commands and vehicle responses during entry and PD. First consider the nominal case. The entry phase (NPCG segments 1 and 2) lasts approximately 290 s. When the G&C is initialized at time zero, the vehicle is at an approximately 1° angle of attack. The flap controller brings the vehicle down to the nominal -6° angle of attack in just under 50 s, with some overshoot, but this occurs at very high altitudes and low dynamic pressures where the flap effectiveness is relatively low. The vehicle follows the nominal command for the rest of entry, with a small increase at TAEM (approximately 210 s). PDI and the augmented gravity turn occurs at 290 s, and the change in angle of attack command to close to 0° is evident.

Now consider the dispersed case in Fig. 7. It can immediately be seen that the angle of attack commands are "stair-stepping" during most of NPCG phase 1, starting at the nominal -6°, increasing to -4°, before settling at -8°. This is indicative of the NPCG attempting to estimate the local density with the IMU axial and normal accelerations a described in Section II.A.3. Towards the end of this phase, beginning at approximately 165 s, the NPCG angle of attack command hits its limit of -9.5°, which has been selected to mitigate flow impingement on the payload (recall that this design does not carry a backshell). This is close to the effective control authority of the flaps, and the "bouncing" or oscillatory motion seen in this period is a result of approaching these limits. Nevertheless, the TAEM phase beginning at 205 s is able to recover, and despite a relatively large overshoot, the angle of attack commands stay near -2°. During PD at 290 s, the angle of attack command is initially zero, and begins to drift more negative, a result of the NPCG attempting to compensate for engine dispersions such as varying peak thrust, Isp, and startup transients. Despite all of these issues, the vehicle lands on target and with expected propellant usage.

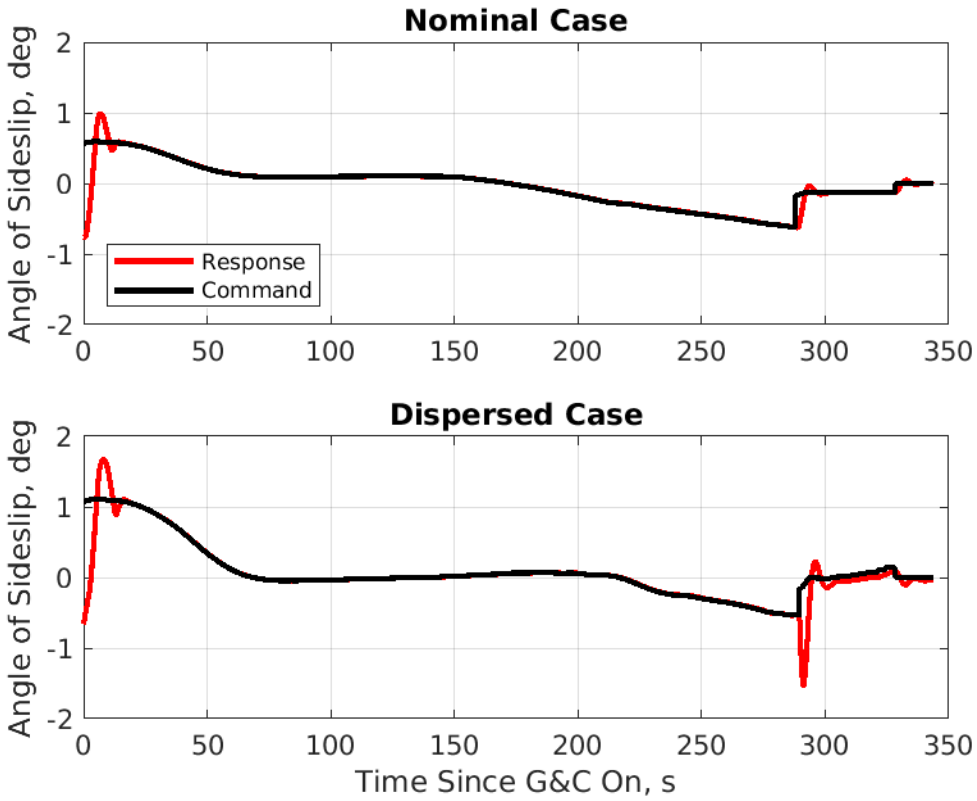

Fig. 8. Nominal and dispersed angle of sideslip commands and responses during entry and PD.

Fig. 8 shows the nominal and dispersed angle of sideslip commands and responses during entry and PD. Angle of sideslip commands are handled differently than angle of attack in the NPCG. Specifically, the angle of sideslip command is defined as

$$\beta_C = k\Delta\varphi \tag{4}$$

where k is a gain selected by the user and $\Delta\varphi$ is the azimuth error (difference between current azimuth and azimuth to the landing site target). This means that the azimuth error, which is directly correlated to crossrange error, can be nulled out across the entire entry portion of the trajectory. This also means that the sideslip command can be computed

continuously and need not be computed at the NPCG call rate. Since the vehicle considered here is a low L/D with an insignificant dihedral effect, the resultant sideslip command is very small (usually between ±5.0°). This can be observed in both the nominal and dispersed cases shown in Fig. 8. Note the change in command to close to 0.0° towards the end of the trajectory. This corresponds to PD and the small sideslip command is the result of the augmented gravity turn. The final change in command to exactly 0.0° is the PD throttle-down phase.

The downward spike in actual sideslip angle just prior to 300 s in the dispersed case is primarily caused by the propulsion startup dispersions, namely, the fact that in dispersed cases the eight main engines start at slightly different times and have slightly different startup transient rates (see Table 3). The main engines quickly recover, however, and the vehicle is able to follow the command relatively closely.

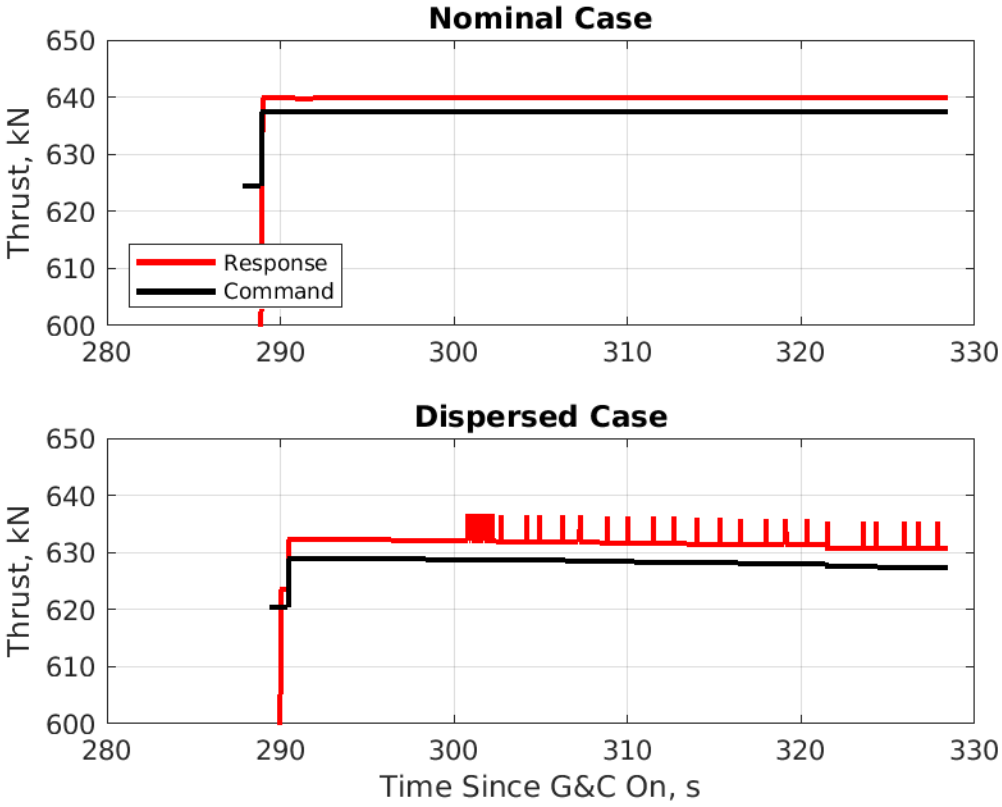

Fig. 9. Nominal and dispersed thrust commands and total thrust responses during PD main phase.

Fig. 9 shows the nominal and dispersed net thrust commands and total thrust responses during the PD main phase. First, note that the *x*-axis scale on these plots are so that the behavior during the PD main phase is readily observable, and the thrust startup from 0.0 kN is cut off. In the nominal case, it can be seen that despite a small offset in commanded vs. actual thrust, the thrust profile is a steady ~80% of full throttle, indicating that the nominal trajectory is closely flying the design trajectory. In the dispersed case, several things are readily observed. First, numerous spikes in the thrust can be seen through the PD main phase. These are roll-axis RCS firings designed to maintain a zero roll angle throughout this phase. Second, the net thrust is lower than that of the nominal case. It has been observed that in dispersed cases, when the NPCG commands an earlier engine start time than the target, the engine throttle is lowered. Conversely, later engine start times correspond to higher throttles. Third, a small downward slope in the thrust profile can be seen. All of these behaviors are indicators that the dispersions introduced to the trajectory, such as the 1% dispersion on engine thrust (see Table 3), are compensated for and flown out by the G&C.

V. Summary

A fully generalized, flexible, and robust user programmable numerical predictor-corrector targeting guidance, or NPCG, has been presented. The NPCG is an extension of an NPC algorithm developed for the Mars Surveyor Program 2001 Missions. Details of the underlying NPCG algorithms were discussed, and NPCG capabilities were demonstrated

using a human-scale low L/D Mars lander simulation. It is expected that the NPCG software will continue to be tested with different spaceflight missions, including other human-scale Mars landers and human-scale Lunar landers. Continual improvements to the NPCG are also anticipated, including leveraging multi-threaded computer processing capabilities.

Acknowledgements

The authors thank Dr. Eric Queen, Dr. Scott Striepe, and Dr. Justin Green (Atmospheric Flight and Entry Systems Branch, NASA LaRC) for insightful discussions and recommendations regarding application of the NPCG to the human-scale Mars EDL case.

References

[1] Cianciolo, A. D., and Powell, R. W., "Entry, Descent, and Landing Guidance and Control Approaches to Satisfy Mars Human Mission Landing Criteria," AAS-17-254.

[2] Powell, R. W., "Numerical Roll Reversal Predictor-Corrector Aerocapture and Precision Landing Guidance Algorithms for the Mars Surveyor Program 2001 Missions," AIAA 98-4574.

[3] Fraysse, H., Powell, R., Rosseau, S., and Striepe, S., "CNES-NASA Studies of the Mars Sample Return Orbiter Aerocapture Phase," 51st International Astronautical Congress, 2-6 October, 2000, Rio De Janeiro, Brazil, IAF-00-A.6.05.

[4] Moore, T. E., "Space Shuttle Terminal Area Energy Management," November 1991, NASA TM 104744.

[5] Klumpp, A. R., "Apollo Lunar-Descent Guidance," Charles Stark Draper Laboratory of the Massachusetts Institute of Technology, Cambridge, MA, 1971, R-695.

[6] Sostaric, R. R. and Rea, J. R., "Powered Descent Guidance Methods for the Moon and Mars," AIAA 2005-6287.

[7] Lugo, R. A., Karlgaard, C. D., Powell, R. W., and Cianciolo, A. D., "Integrated Flush Air Data Sensing System Modeling for Planetary Entry Guidance with Direct Force Control," AIAA 2019-0663.

[8] Lugo, R. A., Shidner, J. D., Powell, R. W., Marsh, S. M., Hoffman, J. A., Litton, D. K., and Schmitt, T. L., "Launch Vehicle Ascent Trajectory Simulation Using The Program to Optimize Simulated Trajectories II (POST2)," AAS 17-274.

[9] D. E. Cornick, R. Stevenson, G. L. Brauer, and R. T. Steinhoff: "Program to Optimize Simulated Trajectories (POST)." MCR-71-781, prepared under Contract NAS1-10811. Martin Marietta Corporation, Denver, Colorado, 1971.

[10] G. L. Kessler: "Generalized N-Phase Trajectory Program (UD-213)." Martin Marietta Corporation, Denver, Colorado, January 1971.

[11] W. E. Wagner and A. C. Serold: "Formulation on Statistical Trajectory Estimation Program." NASA CR-1482. Martin Marietta Corporation, Denver, Colorado, January 1970.

[12] Cianciolo, A. D., and Polsgrove, T. T., "Human Mars Entry, Descent, and Landing Architecture Study Overview," AIAA SPACE 2016, 13-16 September 2016, Long Beach, CA, 10.2514/6.2016-5494.